Laser capture microdissection of the maternal-fetal interface

A Master's project report submitted to the faculty of

San Francisco State University

In partial fulfillment of

the requirements for the degree

Master of Science

in

Cell and Molecular Biology

Emphasis in Stem Cell Research

By

Oliver Oliverio

San Francisco, California

May, 2015

CERTIFICATION OF APPROVAL

I certify that I have read *Laser capture microdissection of the maternal-fetal interface* by Oliver Oliverio, and that in my opinion this work meets the criteria for approving a Master's project submitted in partial fulfillment of the requirements for the degree: Master of Science in Cell and Molecular Biology - Emphasis in Stem Cell Research at San Francisco State University.

_____

Scott W. Roy, Ph.D., Professor of Biology
San Francisco State University

_____

Carmen Domingo, Ph.D., Professor of Biology
Director, CIRM Bridges Program
San Francisco State University

_____

Susan Fisher, PhD. Professor
Principal Investigator, Department of Obstetrics,
Gynecology, & Reproductive Sciences
University of California, San Francisco

Laser capture microdissection of the maternal-fetal interface

Oliver Oliverio

San Francisco, CA

2014

Cytotrophoblasts (CTBs) are the major cell types of the placenta, an organ that mediates nutrient transfer and gas exchange between the mother and fetus. Malformation and misregulation between CTBs leads to pregnancy complications like preeclampsia and preterm birth. To understand possible molecular mechanisms between trophoblast populations (TPs), we performed laser microdissection (LMD) on the placental tissue, isolating these compartments: syncytial, column, and invasive CTBs. We subsequently performed microarray analysis and employed a non-linear principal components analysis (PCA) approach for determining differentially expressed genes (DEGs) between CTB types. Our PCA results were biologically verified using immunohistochemistry, immunoblotting, and confocal microscopy. Using this methodology, we've discovered two potential biomarkers for placental development, cannabinoid receptor-1 (CNR1) and neurotensin (NTS). These proteins are endogenously expressed in the brain and intestine. However, its functions have yet to be explored in the placenta.

I certify that the abstract is a correct representation of the contents of this project

_____

Chair, Master's Project Committee Date

DEDICATION

This thesis is dedicated to my mentors Matthew Gormley and Scott Roy. They have inspired and encouraged me to push the limits of science and programming to the best of my ability. In doing so, they have helped me grow to be a better researcher, and more importantly, a better scientist. Without them, this work would not have been possible.

ACKNOWLEDGEMENTS

I would like to thank Dr. Domingo from the CIRM Bridges Master's Program for her advice, encouragement, and support. I would also like to thank Dr. Susan Fisher for providing me the opportunity to pursue this project. I would like to thank the members of Susan's lab, especially Mirhan Kapidzic for preparing and providing samples. Lastly, I would like to thank my friends and family for supporting me in this scientific venture. This master's project was supported by the University of California San Francisco, California Institute for Regenerative Medicine Bridges Master's Training Grant (TB1-01194) and Department of Biology at San Francisco State University.

TABLE OF CONTENTS

LIST OF FIGURES

Introduction

During nine months of gestation, the human fetus is unequivocally reliant on the placenta[1]. The importance of this organ is highlighted by veneration given by indigenous cultures ranging from Aboriginals to the Kwakiutl Indians of British Columbia. However, its lifespan is short lived. So why is such a transient organ so revered? Many cultural explanations involve superstition with regards to its magical prowess[2]. But few have considered its necessary biological functions for the developing fetus.

Harland Mossman, a comparative placentologist, reduced the placenta's definition to a "fusion or apposition of fetal membranes to uterine mucosa for physiological exchange[3]." However, this definition underrates the vast molecular mechanisms involved in this "fusion" process, most of which remain largely unknown. Furthermore, this overlooks the perplexing properties of the placenta being a chimeric organ, as well as an endocrine modulator. Drawing from multiple pathways ranging from metabolic changes to immunological intercommunications, the placenta is indeed a jack-of-all trades organ.

Its multifaceted functions are accomplished by three the major cell types the placenta. These cytotrophoblast (CTB) populations (TPs) include invasive cytotrophoblasts (iCTBs), column cytotrophoblasts (CCs), and syncytiotrophoblasts (SynTs). These three TPs fulfill three main functions, blood perfusion, fetal-uterine attachment, and establishment of a nutrient exchange surface, respectively. A proper functioning placenta relies heavily on proper differentiation and formation of these TPs. Malformation will lead to severe pregnancy etiologies such as preeclampsia. This is especially true in the invasive population.

Invasion: A necessary assault on maternal vessels

Abnormal trophoblast differentiation leads to pathogenesis of development diseases such as preeclampsia. This etiology is characterized by hypertension, proteinuria, and edema for the mother, as well as growth restriction for the fetus. Generally, interstitial invasion of the uterus is shallow, and endovascular invasion of maternal blood vessels is incomplete. Molecularly, as CTBs differentiate to iCTBs, they switch from an epithelial cell type to an endothelial type expressing vascular-endothelial cadherin, VCAM-1 and PECAM-1. Without proper switching towards endothelial features, iCTBs do not remodel vessels required for proper blood perfusion[4]. In fact, they are found significantly distant from these vessels. And if they are found, this incomplete remodeling is limited to vessels spanning the superficial decidua. Another feature owing to the ineffectiveness of preeclamptic iCTBs is their tendency to remain as large aggregates within the uterine wall, rather than as smaller clusters and single cells performing their job of invading spiral arterioles. This is evident in strong staining for E-cadherin in iCTBs of preeclamptic tissue[5].

Signaling at a distance: The neuroendocrine features of the placenta

The floating villi is immediately adjacent to maternal blood. Such configuration lends itself to fetal-maternal signaling mechanisms during gestation. There are well known placental hormones that regulate fetal and maternal metabolism. Maternal pituitary growth hormone (GH) is gradually replaced by placental GH during the second trimester. These are produced by the SynT population, and its increase in intermediary metabolism allows the fetus to intake more glucose and amino acids for proper development[6]. In addition to metabolism regulation, the placenta is also a source of neuropeptides. These include vasoactive intestinal polypeptide and

neuropeptide Y{Reis:2001uf}. Other endocrine features have yet to be explored given this study's microarray data of this TP. Neurotensin, a neuropeptide involved in smooth muscle contraction and relaxation, and found to be upregulated in SynTs, was a viable candidate for immunolocalization.

This work will describe the discovery of two potentially essential proteins expressed in iCTBs and SynTs, cannabinoid receptor-1 (CNR1) and neurotensin (NTS), respectively. The functions of these proteins are virtually unknown in the placenta. However, they are expressed in crucial cell types in charge of proper placental function. This work will also describe a novel informatics approach in arriving to these two proteins, as well as contextualizing data into biologically meaningful results. Principal components analysis (PCA) and Circos programming have been used to guide experimentation and introduce new hypotheses in light of this novel approach of contextualizing big data.

MATERIALS AND METHODS

2.1 Laser capture microdissection of placental tissue.

Laser microdissection[7] (LMD) will be used to isolate TPs from second trimester placental tissue. Placental tissue was dissected and prepared by Mirhan Kapidzic, a specialist in placental tissue processing and embedding. Using a Leica CM3050 S, cyrosections were performed at 20 µm thick slices onto PET-membrane slides. Tissue sections were stained with toluidine blue, an acidic stain that marks nucleic acids allowing for visualization of TPs. Slides were placed in a dry ice chilled slide box until needed for dehydration. An ethanol gradient at concentrations of

75%, 95%, and 100% was used to dehydrate tissue slides. Slides were then air dried and then placed onto the dissection scope stage in preparation for laser microdissection.

Using a PC supplied with Leica Application Suite software, collection well placement and laser calibration was done for proper collection. Placenta compartments or regions of interest (ROI) were then outlined by hand and chosen for laser isolation. Coupled with the laser dissection scope, these outlines are cut and dropped into wells containing RNA lysis buffer for further RNA isolation.

RNA was extracted using RNAeasy Micro kit (Qiagen). Isolated RNA was then quantified using a Nanodrop fluorospectrometer, and quality was assessed using Agilent's RNA 6000 Pico bio-analyizer. This determines RNA integrity by sending charged molecules (DNA/RNA) through an integrated electrical circuit comprised of glass microchannels. RNA molecules are driven by electrophoresis, and with an intercalating dye, can be measured and quality assessed by an RNA integrity number (RIN) ranging from 1 to 10. A score of 1 suggests RNA is degraded, while 10 suggests all RNA is intact. Samples with RNA integrity scores greater than 7 will proceed to microarray hybridization at the Gladstone Institute.

2.2 Microarray analysis and gene expression of placental cell types

Microarray hybridization of the cDNA sample to probes was done at the Gladstone Institute, and data analysis was done using R, Bioconductor, Affytools, and other freely available R software packages. Raw CEL files were imported and summarized using Affymetrix's Expression Console software. Gene level analysis and RMA normalzation was also performed using this software. The resulting dataset are CHP files or summarized intensity files following normalization. These were then exported with gene annotations to excel spreadsheets for further

processing. Using excel, genes were filtered by median normalization. Any gene containing a median intensity less than the median of the entire gene set was excluded. This removes technical noise due to probes with weak signals that essentially have an effect in the statistical analysis of determining significant genes. The resulting table was exported to a limma file for differential expression hypothesis testing. Limma was performed using Bioconductor package "oneChannelGUI," and the Benjamini–Hochberg procedure or false discovery rate (FDR) was used to account for multiple hypothesis testing. The resulting table is a list of differentially expressed (DE) genes of a placental cell population sorted by p-value.

2.3 Generation of differential expression gene lists using Principal Components Analysis

In addition to traditional Limma methodology for determining differentially expressed genes, PCA was also used for clustering gene expression data and generating DE gene lists [8]. Using Excel, raw intensity values of probes were median normalized and centered to zero, and principal components were calculated using R's built in "princomp" function. Principal component scores were appended to each gene and sorted in Excel. Color coding the raw intensity values while sorting by PCA score demonstrates the separation of cell or sample types. For example, sorting genes in ascending order of principal component 1 shows the top genes expressed in the syncytium, whereas descending order displays upregulated genes in invasive CTBs. Biplots show the direction of the eigenvectors where there is the most variation in gene expression data. These were constructed using Origin Pro as well as R's built in "biplot" function.

2.4 Circos figure plotting of microarray data and Ingenuity Pathway Analysis (IPA)

Circos[9] was installed on a linux and Mac OS X based system (supplied with Perl, a high level programming language package) via terminal, a command line interface that allows for text-based access to the operating system. Additional Perl modules needed for graphics and text processing were manually installed. Additional scripts were written to ease the Circos command line workflow, and the configuration files that Circos takes in as input were written using text editors Vim and Sublime.

Configuration files were created using custom built Perl scripts. The major configuration files in a Circos plot are gene-names.config, histogram.config, and links.config. The histogram.config configuration file consists of gene expression data with track informations in column 1 followed by intensity value in column 2. Gene-pathway interactions determined by IPA were programmatically formatted as a Circos input [10]. An interaction determined by IPA is structured as ordered pairs where one pair consist of "gene a," followed by "pathway a," the pathway that this gene overrepresents. These pairs are listed in a links text file as a parameter for Circos to plot.

2.5 Immunolocalization and confocal microscopy of cannabinoid receptor 1 (CNR1) and neurotensin (NTS)

Placental tissue blocks containing these areas were prepared by PFA fixation and sucrose gradient. These blocks were sectioned at 30 μm in thickness onto positively charged glass slides and stored in -20ºC until needed for immunolocalization. Slides were blocked with blocking buffer (3% BSA, 0.1% Triton-X, 0.05% Tween 20, 0.1% cold fish skin gelatin and Ca/Mg free PBS) for 1hour at 4ºC. Slides were then incubated with rabbit anti-CNR1 (Abcam, cat. no.

ab23703), rabbit anti-NTS (Abcam, cat .no. AB5496), mouse anti-HLA-G, and rat anti-CK primary antibodies overnight at 4ºC. The next day, slides were washed three times in cold PBS (Ca++/Mg free) for 10min. Secondary antibodies against rabbit, mouse, and rat (Jackson) and Phalloidin 633 were diluted in room temperature (RT) PBS and added to slides. These were incubated for 45 minutes in RT. Slides were then washed again with cold PBS, and anti-fade with dapi was applied and coverslip sealed. Slides were stored in the dark at 4ºC until confocal imaging. Confocal imaging was done using a Leica TCS SP5 Confocal Microscope with Leica Application Suite software. A step size of 1.5µm and a resolution of 2048 x 2048 pixels were used to capture raw stacked images. We used Volocity imaging software to render 3D images of the NTS expression villi surface, as well as orthogonal projections to demonstrate specific cellular localization of CNR1. Confocal images were stacked in Adobe Photoshop.

2.6 Immunoblotting of CNR1 and NTS

To test for CNR1 nuclear protein expression, protein was extracted from basal plate. Fetal brain tissue was used as a positive control. These tissues were homogenized for 2 min in NE-PER (Life Technologies) following manufacturer protocol. To test for NTS expression, floating villi was extracted from the fetal side of the basal plate and homogenized in M-PER. Fetal intestine was used as a positive control. Samples were spun at the highest setting and the supernatant containing protein lysates were stored in -80 until needed for immunoblotting. Protein concentration was determined using UV-1700 UV-Vis Spectrophotometer (PharmaSpec).

After determining protein concentration 100µg of each sample was prepared for SDS-PAGE. Samples were doubly reduced with 200mM DTT and 3% beta-mercaptoethanol, and

boiled for 5 minutes. Samples were then run on a 4-12% gradient polyacrylamide gel at 100V. These were then laterally transferred to nitrocellulose membranes using a Bio-Rad Semi-dry transfer blotter. Membranes were then blocked in 5% blocking buffer in PBS containing 0.1% Tween 20 (PBS-T for 40 minutes at room temperature with gentle shaking. We incubated these membranes with rabbit anti-CNR1 primary antibody (Abcam, cat. no. ab23703) and mouse beta-actin primary antibody at 4ºC overnight. The following day, membranes were washed three times with PBS-T and incubated with rabbit (Jackson, cat. no. 711-035-152) and mouse (Jackson, cat. no. 315-035-003) horse-radish peroxidase (HRP) congugated secondaries for one hour at room temperature. Membranes were washed again three times and prepared for enhanced chemical luminescence (ECL) and signal exposure and detection on x-ray film.

2.7 Invasion assay of trophoblasts treated with (R)-methanandamide

A 2:1 concentration of matrigel was thawed on ice until ready for coating of membrane slides. Matrigel was dispersed evenly onto transwell membranes with 8.0µm pores and then incubated for 15 min at 37ºC. Second trimester trophoblast cells were prepared by our placental dissection specialist, Mirhan Kapidzic, and plated onto matrigel coated transwel plates as well as flat bottom 12 well plates.

The concentrations of (R)-methanandamide used were adapted from a neuronal cell signaling assay by Lume et. al [11]. A 10nM concentration of (R)-methanandamide was used for a low dose condition, while 100nM was used for a high dose condition. Our negative control consisted of media containing Tocrisolve, the solution in which anandamide was dissolved.

Cells were imaged every 24 hours and finally fixed with 1% PFA after 36 hours. These were then stained with cytokeratin-7 and CNR1 (Abcam, cat. no. ab23703). Membranes were

cut from the transwells, transfered to glass slides, and sealed with Vectashield. CK7 positive projections and invaded CTBs were counted and imaged between each condition. Cell death was assessed by Tunnel assay (Roche, 12 156 792 910), and cell proliferation was assessed using by Edu assay (LifeTechnologies, C10637) according to manufacturer protocol.

RESULTS

3.1 A modern novel approach to isolating TPs and obtaining DEGs.

Representative genes or DEGs for each TP were obtained in this microarray comparative analysis. NTS is among the top 5 genes in the syncytial population (**Fig 1b**), and CNR1 is differentially expressed in the invasive population (**Fig 1c**).

A.

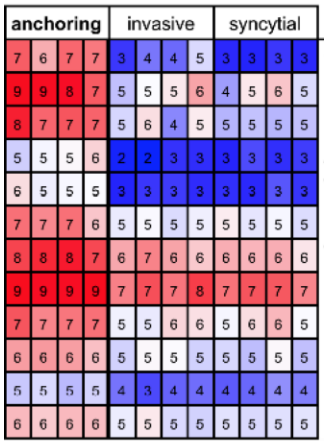

Symbol	Title	Δ
OXGR1	oxoglutarate (alpha-ketoglutarate) receptor 1	15
ITGB6	integrin, beta 6	10
NLRP2	NLR family, pyrin domain containing 2	6
ACAN	aggrecan	5
VIT	vitrin	5
GPR37	G protein-coupled receptor 37 (endothelin receptor type B-like)	3
VLDLR	very low density lipoprotein receptor	3
PPARG	peroxisome proliferator-activated receptor gamma	3
CCRN4L	CCR4 carbon catabolite repression 4-like (S. cerevisiae)	3
RFK	riboflavin kinase	3
RAB30	RAB30, member RAS oncogene family	2
DLX6	distal-less homeobox 6	2

B.

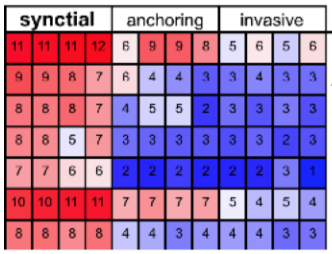

Symbol	Title	Δ
GH2	growth hormone 2	39
AREG	amphiregulin	37
SLC27A2	solute carrier family 27 (fatty acid transporter), member 2	28
CPS1	carbamoyl-phosphate synthase 1, mitochondrial	27
NTS	neurotensin	26
SVEP1	sushi, von Willebrand factor type A, EGF and pentraxin dom	26
MEOX2	mesenchyme homeobox 2	23

C.

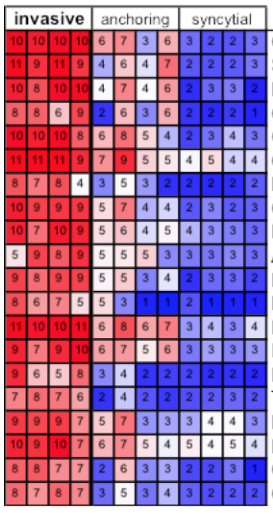

Symbol	Title	Δ
CHRDL1	chordin-like 1	160
SLPI	secretory leukocyte peptidase inhibitor	105
PRL	prolactin	73
CXCL9	chemokine (C-X-C motif) ligand 9	72
GZMA	granzyme A (granzyme 1, cytotoxic T-lymphocyte-associated serine esterase 3)	69
OMD	osteomodulin	65
KLRC1	killer cell lectin-like receptor subfamily C, member 1	54
CFH	complement factor H	50
RXFP1	relaxin/insulin-like family peptide receptor 1	50
ANKRD1	ankyrin repeat domain 1 (cardiac muscle)	49
RORB	RAR-related orphan receptor B	46
KLRC3	killer cell lectin-like receptor subfamily C, member 3	42
HLA-DRA	major histocompatibility complex, class II, DR alpha	39
IL1RL1	interleukin 1 receptor-like 1	37
FGG	fibrinogen gamma chain	30
TRPC4	transient receptor potential cation channel, subfamily C, member 4	30
PROK1	prokineticin 1	28
NKG7	natural killer cell group 7 sequence	28
C13orf33	chromosome 13 open reading frame 33	27
CNR1	cannabinoid receptor 1 (brain)	26

Figure 1. Microarray analysis of LMD isolated TPs from second trimester placental tissue. Significantly active genes in the column, syncytial, and invasive TPs, respectively (A-C).

DEGs for each TP were also obtained via PCA. The biplot associates principal components to eigenvectors that separate each TP according to their variation in their microarray data. Eigenvectors show where the maximum variation lies, and representative genes are highlighted in each biplot quadrant (**Fig 2A-D**). NTS and CNR1 are highlighted in their respective placental compartments.

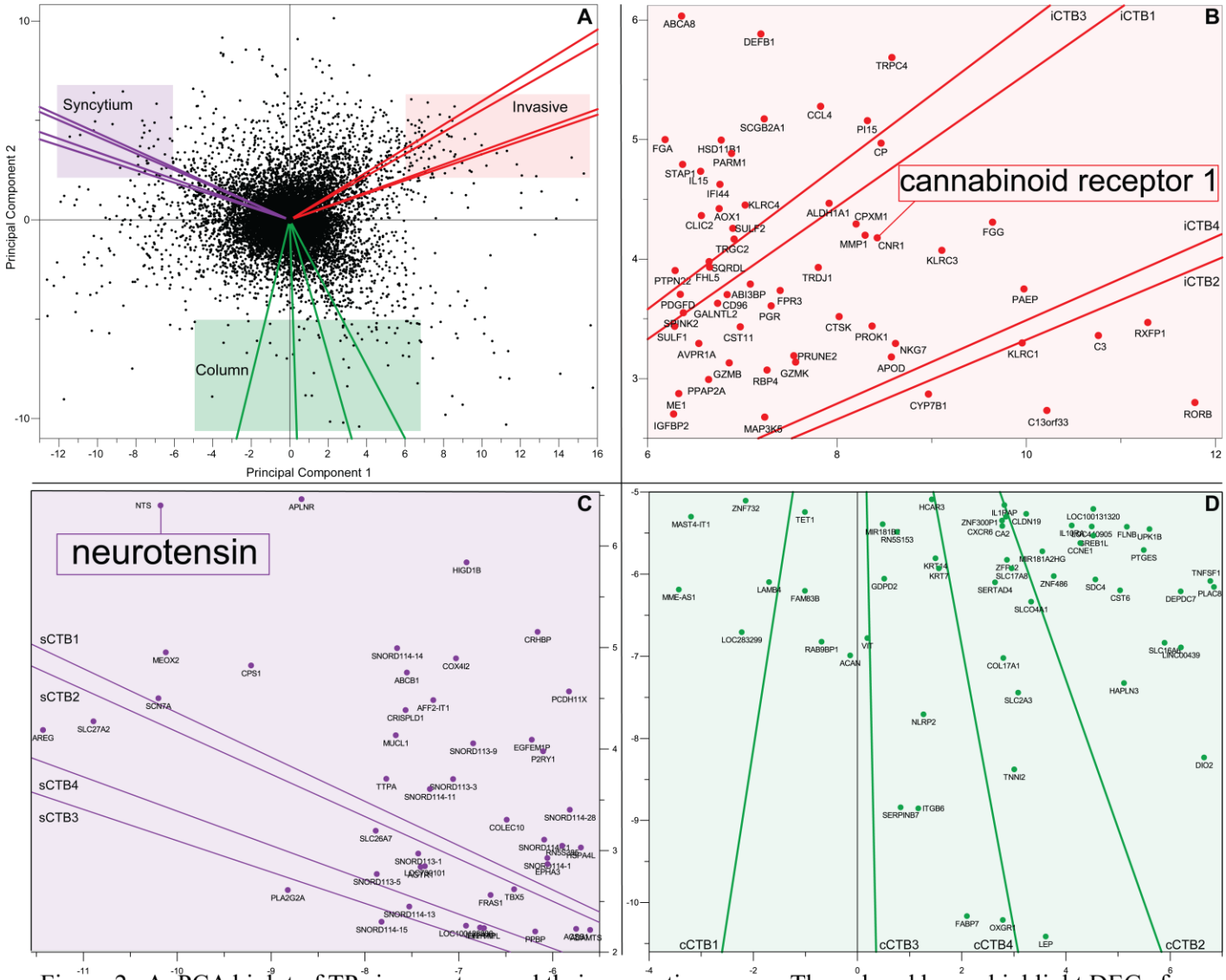

Figure 2. A. PCA biplot of TP eigenvectors and their respective genes. The colored boxes highlight DEGs for each TP. B. Invasive trophoblast PCA highlighting CNR1. C. Syncytial PCA highlighting NTS. D. Cell column PCA.

3.1 NTS is localized on the syncytial surface of floating villi.

As our PCA microarray methodology suggests, NTS is predicted to be expressed in the syncytial TP. Our confocal microscopy results confirm this. The Z-stack image of immunolocalized NTS show it to be expressed in the floating villi. Its expression demonstrates a vesicular pattern immediately adjacent to maternal blood (**Fig 3**), suggesting a possible endocrine function given by this protein.

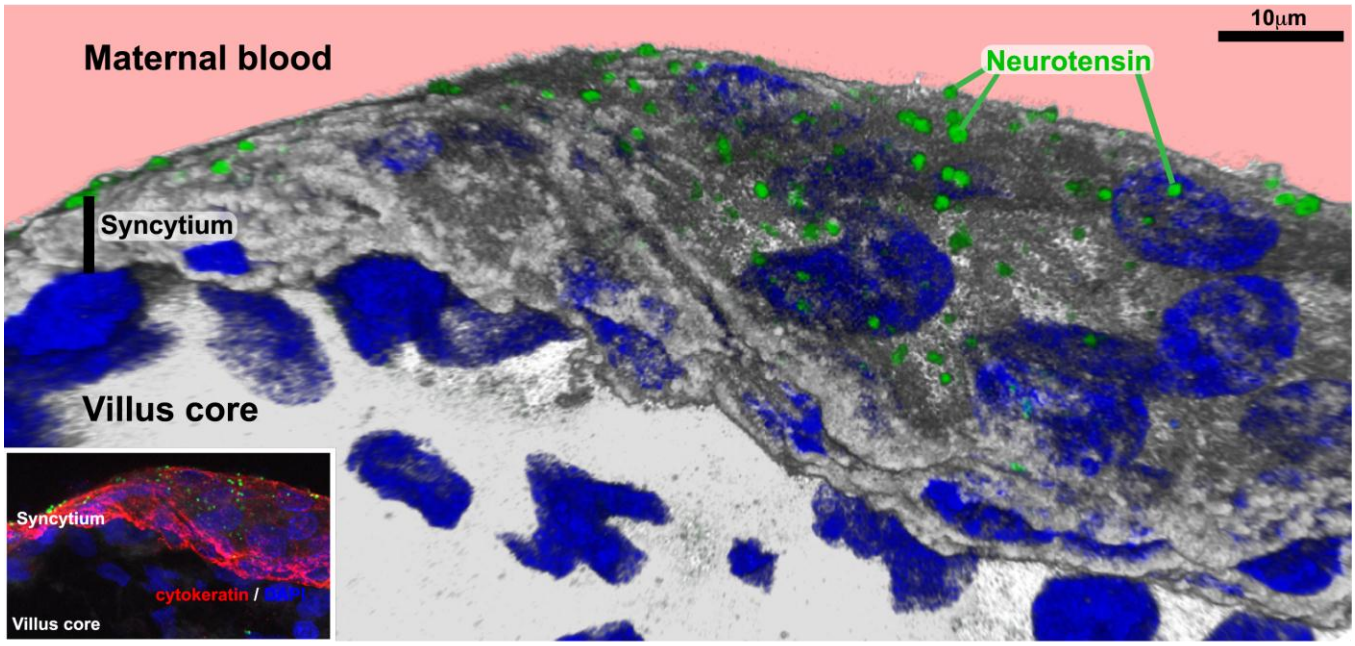

Figure 3. 3D rendering of the syncytium expressing NTS in a vessicular pattern immediately adjacent to maternal blood. The inset shows the Z-stack max projection used for rendering.

3.2 CNR1 is localized in the nucleus of invasive CTBs.

CNR1 is predicted to be expressed in the invasive TP as given by our microarray PCA analysis. Immunolocalization and confocal imaging also confirms this. At high resolution, CNR1 expression can be resolved at the cell compartment level. The 3D rendering of our Z-

stack confocal images shows that CNR1 is expressed in the nucleus of iCTBs, but also in the membranes of non-CTB populations (**Fig 4**.)

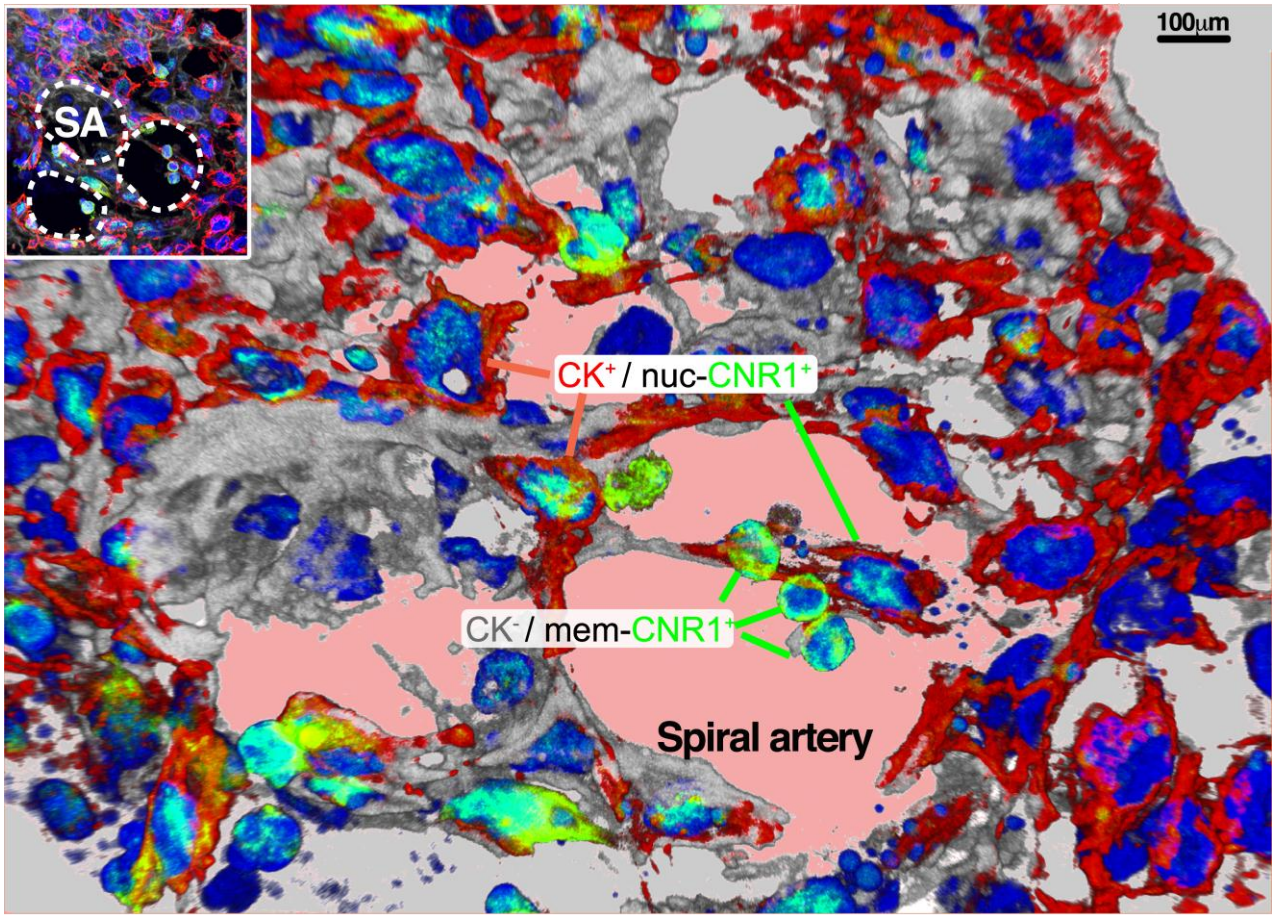

Figure 4. 3D rendering of a spiral artery containing CNR1 within the nuclei of invasive cytotrophoblasts. Membranous CNR1 is observed in the non-trophoblast population

3.3 Immunoblotting of NTS and CNR1 in isolated 2nd trimester placental tissue.

Protein extracts of second trimester villi show NTS expression. This protein is expressed at higher levels in villi compared to extracts of basal plate or the maternal-fetal interface (MFI) (**Fig 5a**).

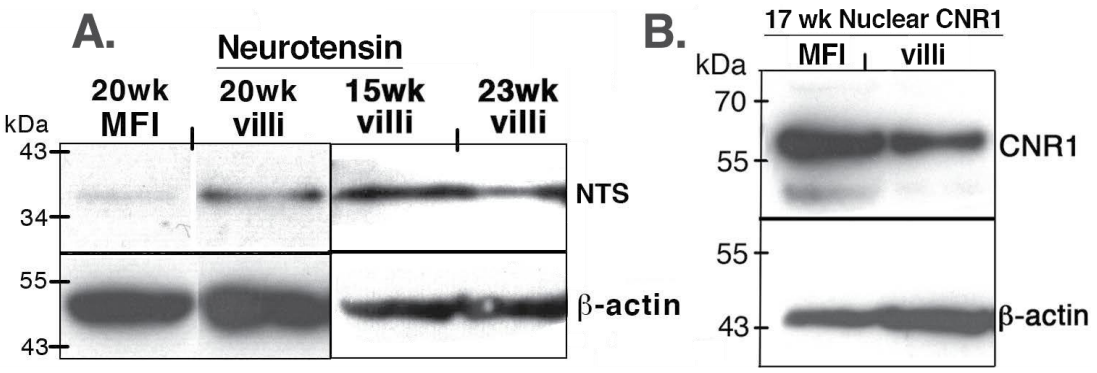

Figure 5. Immunoblots of CNR1 and NTS. A. NTS is expressed at higher levels in the syncytium of villi than the maternal-fetal interface (MFI). B. CNR1 is expressed in the nuclear fraction of MFI protein isolates.

CNR1 Immunolocalization and confocal microscopy suggests nuclear expression within iCTBs. This prompted a nuclear protein extraction method from second trimester tissues. CNR1 expression is observed in the nuclear fraction of protein isolates of the MFI (**Fig 5b**).

3.2 Invasion increases in (R)-methanandamide treated CTBs.

The average number of projections in our control was 495 as opposed to 1108 in our treated condition of 10nM (R)-methanandamide. We observed a significant increase in invasion in anandamide treated CTB culture (**Fig 6**). The 100nM condition resulted in cell death resulting in few or no projections.

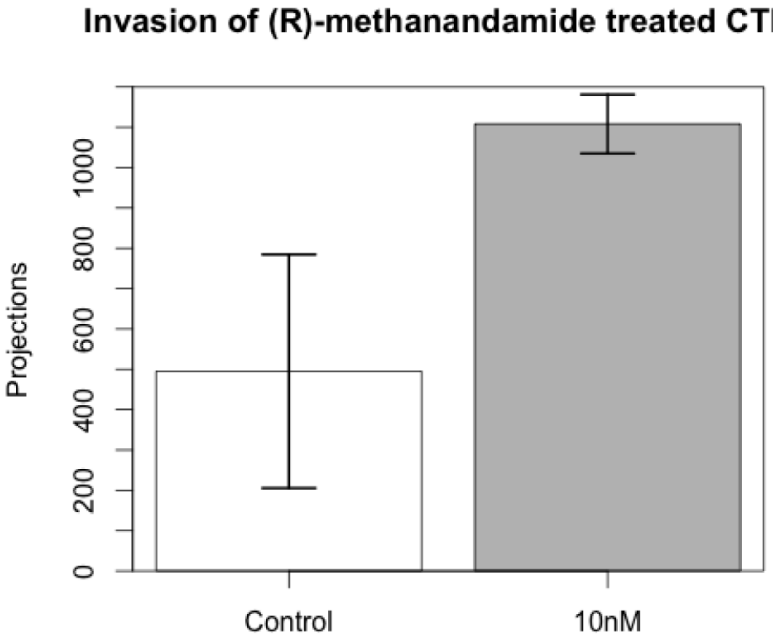

Figure 6. Invasion assay barplot of projections from (R)-methanandamide treated CTB culture. A concentration of 10nM to CTB culture results in a significant difference in invasion ($p = 0.023$).

DISCUSSION

Current understanding of CTB invasion is limited, and prevailing informatics and wet-lab methods for studying this process are constantly evolving. Microarray technology has been the forefront of determining significant differential expression between cell populations, but the vast range of data analysis methods continue to identify new routes of experimentation. This has been especially true in studying the perplexing process of CTB invasion. Our PCA microarray methodology uncovered a possible key protein, CNR1, within iCTBs.

In addition to PCA, Circos, an emerging data analysis tool has been employed to contextualize microarray data. This can be programmed to uncover gene-gene or gene-pathway relationships that would have otherwise been hidden within big data. IPA generates tables of

significant pathways given a ranked gene list, usually from comparative microarray analysis[10] (**Fig 7**).

Pathways	Sample	-log(p-val)	Ratio	z-score	Genes							
Colorectal Cancer Metastasis Signaling	cCTB	1.36	0.0478	2.828	FOS	NOS2	TGFB1	MMP2	TLR3	MMP12	TGFB2	JAK1
Colorectal Cancer Metastasis Signaling	iCTB	2.02	0.0348	2.828	TLR4	JUN	PROK1	TLR7	WNT5A	PRKACB	MMP1	PIK3CG
Role of Pattern Recognition Receptors in R	iCTB	3.83	0.0672	2.646	TLR4	C1QC	TLR7	IL1B	C5AR1	C3AR1	PIK3CG	C1QA
ILK Signaling	iCTB	1.55	0.0333	2.449	JUN	PROK1	ITGB8	MYL9	MUC1	PIK3CG		
ILK Signaling	cCTB	1.66	0.0556	2.121	FOS	FLNB	SNAI1	FN1	NOS2	ITGB6	DSP	PXN
IGF-1 Signaling	cCTB	1.86	0.0729	2	FOS	IGFBP1	SFN	PXN	JAK1	IGFBP3	PIK3CB	
Role of Pattern Recognition Receptors in R	cCTB	1.86	0.0672	2	OAS1	TGFB1	TLR3	PRKD3	IFIH1	OAS3	TGFB2	PIK3CB
Nitric Oxide Signaling in the Cardiovascula	iCTB	1.49	0.0426	2	PLN	PROK1	PRKACB	PIK3CG				
Nitric Oxide Signaling in the Cardiovascula	sCTB	2.77	0.0426	1	GUCY1A2	KDR	GUCY1B3	PDE5A				
IGF-1 Signaling	iCTB	3.64	0.0729		JUN	IGFBP4	IGFBP7	IGFBP2	IGFBP5	PRKACB	PIK3CG	
HIF-1-alpha Signaling	cCTB	1.79	0.0707		NOS2	MMP2	SLC2A3	EGLN3	MMP12	SLC2A1	PIK3CB	
TR/RXR Activation	cCTB	1.6	0.0706		PFKP	SLC2A1	PIK3CB	DIO2	SLC16A3	THRB		
Granulocyte Adhesion and Diapedesis	iCTB	5.19	0.0692		C5AR1	C5AR1	CCL13	CCL2	CCL21	CCL23	CCL4	CCL4L1
Human Embryonic Stem Cell Pluripotency	cCTB	1.63	0.0611		BMPR2	INHBA	BMP5	TGFB1	TGFB2	TCF7L2	PIK3CB	NOG
Granulocyte Adhesion and Diapedesis	cCTB	1.59	0.0566		CLDN7	MMP2	ITGA2	MMP12	IL1RAP	IL1R2	CLDN19	SDC4
HIF-1-alpha Signaling	iCTB	2.05	0.0505		JUN	PROK1	EDN1	MMP1	PIK3CG			
TR/RXR Activation	iCTB	1.63	0.0471		ME1	FGA	KLF9	PIK3CG				
Human Embryonic Stem Cell Pluripotency	iCTB	1.57	0.0382		PDGFD	PDGFRA	WNT5A	FGF2	PIK3CG			
G-Protein Coupled Receptor Signaling	iCTB	1.78	0.0315		FYN	CNR1	RGS2	P2RY14	PRKACB	AVPR1A	NPR3	PIK3CG
G-Protein Coupled Receptor Signaling	sCTB	1.31	0.0157		PLCB1	APLNR	PDE5A	AGTR1				
Acute Phase Response Signaling	iCTB	7.56	0.0848	3.162	JUN	MAP3K5	IL1B	CP	FGA	RBP4	FGG	PIK3CG
NF-kappa-B Signaling	iCTB	3.6	0.0552	3	TLR4	TNFRSF1	TNFSF13	TLR7	IL1B	PDGFRA	FCER1G	PRKACB
HGF Signaling	cCTB	2.19	0.0769	2.646	FOS	PRKD3	ITGA2	ELF4	MET	PXN	PIK3CB	ITGA5
Tec Kinase Signaling	cCTB	1.36	0.0541	2.646	FOS	PRKD3	ITGA2	TNFSF10	JAK1	PIK3CB	ITGA5	VAV2
Production of Nitric Oxide and Reactive Ox	iCTB	2.12	0.0398	2.646	TLR4	JUN	TNFRSF1	MAP3K5	APOD	RBP4	PIK3CG	
Cdc42 Signaling	cCTB	1.41	0.0588	2.449	FOS	ITGA2	FNBP1L	HLA-G	DIAPH3	ITGA5	VAV2	
Role of NFAT in Regulation of the Immune	iCTB	1.79	0.038	2.449	JUN	LCP2	FYN	CD3D	FCER1G	PIK3CG		
Leukocyte Extravasation Signaling	cCTB	1.88	0.0576	2.333	F11R	CLDN7	MMP2	PRKD3	ITGA2	MMP12	PXN	CLDN19

Figure 7. Table of significant pathways given by IPA from a ranked microarray DE gene list.

Unfortunately, there is no obvious conclusion can be from this data at a first glance. However, this can be used in conjunction with Circos to give a visual representation of tabular data. With Circos, our comparative mircoarray analysis isn't limited to interpreting differential expression, but expanding this interpretation to possible pathways each gene set may influence (**Fig 8**).

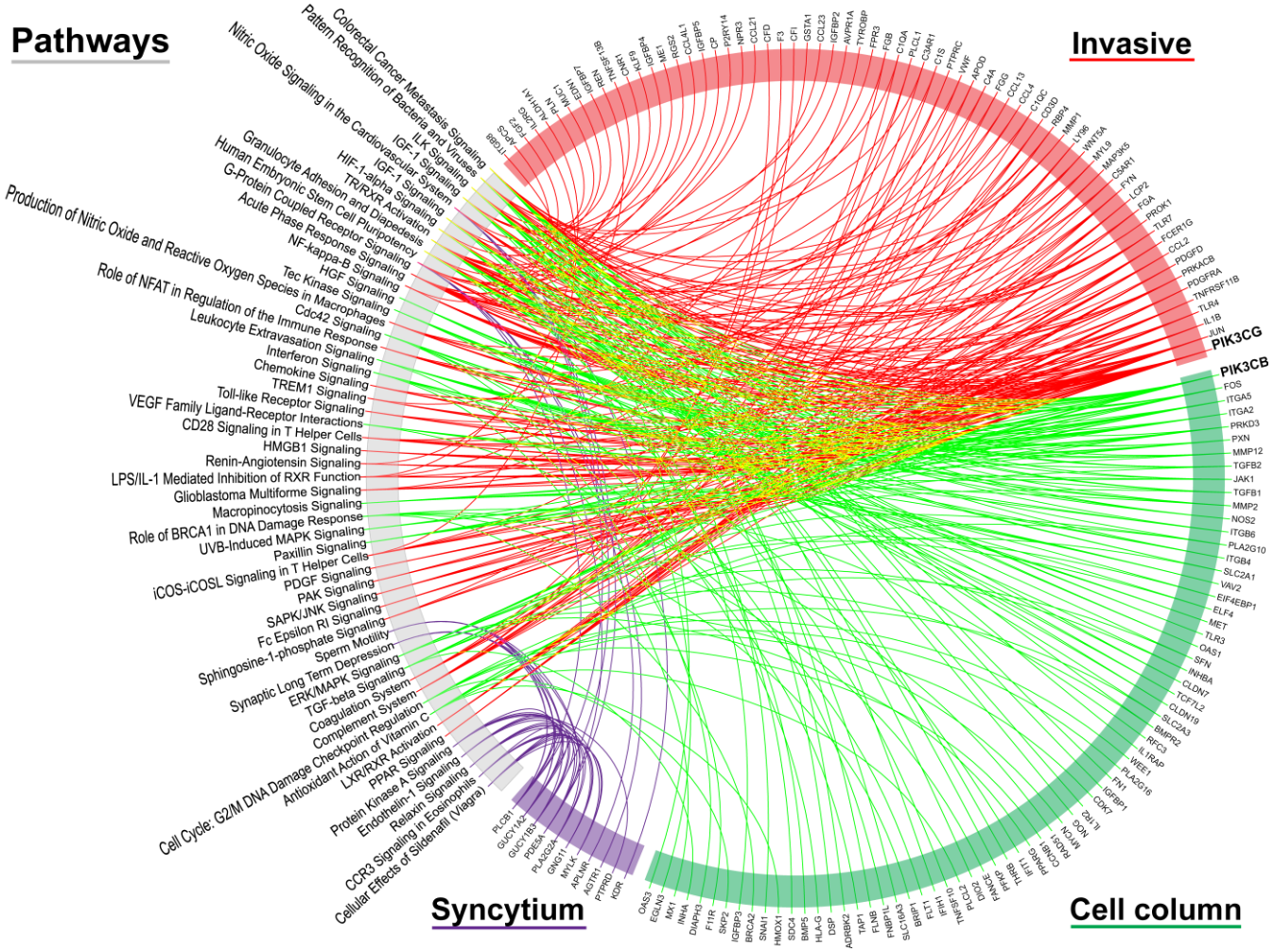

Figure 7. Circular plot of DEGs from the syncytium, cell column, and invasive trophoblast populations linked to their respective pathways. The DEGs of each group are sorted descending according to their number of pathway connections. The pathways are sorted descending according to their number of member genes.

Furthermore, it can be programmed to uncover gene-pathway relationships shedding light on the drivers of differences between cell types. By sorting genes based on the number of pathways connections, we show that two isoforms of the phosphoinositide 3-kinase gene (PIK3CB and PIK3CG) are driving differences between the invasive TP and cell column TP.

These isoforms do appear in our DEG list, but obtains an even greater significance in light of this Circos representation of IPA data.

Although no overrepresented pathway featured NTS, and only one featured CNR1, their expression given by PCA, immunolocalization, and immunoblotting demonstrates unknown functional significance. Much work has been done in mouse to relate adverse effects of cannabinoid signaling to placentation and trophoblast development. *CNR1*$^{-/-}$ mice produced 50% less liters compared to WT. Molecularly, *CNR1*$^{-/-}$ spongiotrophoblasts (SPT) produced less trophoblast specific protein-alpha, suggesting that a defect in forming the SPT compartment[12]. This compartment is analogous to the extravillous invasive CTB population in the human MFI. S.K. Dey also showed that a loss of CNR1 induces preterm birth in mice[13]. Conversely, Fugedi et. al. showed that CNR1 expression is increased in cases of preeclampsia[14].

Our confocal results resolve this observation at the nuclear level. We see nuclear as well as membranous expression of CNR1 in human MFI. Our invasion assay results speak to the notion that a certain concentration of anandamide is needed for proper invasion. This finding suggests that added drug may compensate for the absence of endogenous invasive signals when CTBs are cultured in-vitro. But when the anandamide concentration is above physiological levels , cell death occurs, and invasion is inhibited.

NTS was first isolated from bovine hypothalami[15] and known to stimulate contraction of the rat uterus but relaxation of its duodenum[16]. Its endogenous expression in the placenta is now known given our immunolocalization data, but its functional relevance has still yet to be explored. Nevertheless, its existence in the placenta is intriguing given that this is a non-innervated organ. In light of its expression immediately adjacent to maternal blood, NTS may function as a neuroendocrine peptide in modulating the mother's physiology during pregnancy.

It has implications in hypotension and vasodilation, suggesting a possible mechanism in increasing uteroplacental blood flow required for the growing fetus[17].

CONCLUSIONS

This investigation has revealed new informatic methodologies for discovering placental biomarkers and significant molecules required for CTB invasion and endocrine signaling. Trophoblasts must invade uterine vasculature to establish placenta perfusion, without killing or being killed by the mother. Combined with novel array analysis as well as traditional immonolocalization and immunoblotting techniques, we demonstrate an intimate association between maternal uterine cells and invading trophoblasts expressing nuclear CNR1. Thus, we've identified likely association between endocannabinoid signaling with trophoblast invasion. Pregnancy complications arise when invasion is too shallow, e.g., preeclampsia, or too deep, e.g., accreta, suggesting cannabinoid intake during pregnancy may induce disease. Trophoblasts must further establish hemochorial exchange for nutrition. During the course of her pregnancy, a woman's heart, liver, kidneys and pancreas all grow in size to meet the metabolic demands of viviparity. We also show that a neuropeptide, neurotensin, is expressed on the syncytium. Perhaps this and other neuropeptides signal the hypertrophy of pregnancy.

REFERENCES

1. Burton, G. J. & Fowden, A. L. The placenta: a multifaceted, transient organ. *Philosophical Transactions of the Royal Society B: Biological Sciences* **370,** 20140066 (2015).
2. Long, E. C. The Placenta in Lore and Legend. *Bull Med Libr Assoc* **51,** 233–241 (1963).
3. Mossman, H. W. *Classics revisited: Comparative morphogenesis of the fetal membranes and accessory uterine structures. Placenta* **12,** 1–5 (1991).
4. Red-Horse, K. *et al.* Trophoblast differentiation during embryo implantation and

formation of the maternal-fetal interface. *J. Clin. Invest.* **114,** 744–754 (2004).
5. McMaster, M. T., Zhou, Y. & Fisher, S. J. Abnormal placentation and the syndrome of preeclampsia. *Seminars in Nephrology* **24,** 540–547 (2004).
6. Handwerger, S. & Freemark, M. The roles of placental growth hormone and placental lactogen in the regulation of human fetal growth and development. *J. Pediatr. Endocrinol. Metab.* **13,** 343–356 (2000).
7. Espina, V. *et al.* Laser-capture microdissection. *Nat Protoc* **1,** 586–603 (2006).
8. Yeung, K. Y. & Ruzzo, W. L. Principal component analysis for clustering gene expression data. *Bioinformatics* **17,** 763–774 (2001).
9. Krzywinski, M. *et al.* Circos: an information aesthetic for comparative genomics. *Genome Research* **19,** 1639–1645 (2009).
10. Jiménez-Marín, A., Collado-Romero, M., Ramirez-Boo, M., Arce, C. & Garrido, J. J. Biological pathway analysis by ArrayUnlock and Ingenuity Pathway Analysis. *BMC Proc* **3 Suppl 4,** S6 (2009).
11. Blume, L. C., Eldeeb, K., Bass, C. E., Selley, D. E. & Howlett, A. C. Cellular Signalling. *Cellular Signalling* **27,** 716–726 (2015).
12. Sun, X. *et al.* Endocannabinoid signaling directs differentiation of trophoblast cell lineages and placentation. *Proc Natl Acad Sci U S A* **107,** 16887–16892 (2010).
13. Wang, H., Xie, H. & Dey, S. K. Loss of Cannabinoid Receptor CB1 Induces Preterm Birth. *PLoS ONE* **3,** e3320 (2008).
14. Fügedi, G. *et al.* Increased placental expression of cannabinoid receptor 1 in preeclampsia: an observational study. *BMC Pregnancy Childbirth* **14,** 395 (2014).
15. Carraway, R. & Leeman, S. E. The isolation of a new hypotensive peptide, neurotensin, from bovine hypothalami. *J. Biol. Chem.* **248,** 6854–6861 (1973).
16. Kitabgi, P. & Freychet, P. Effects of neurotensin on isolated intestinal smooth muscles. *Eur. J. Pharmacol.* **50,** 349–357 (1978).
17. Unnikumar, K. R. Human Placenta Contains Neurotensin: Immunohistochemical Evidence. *Biomedicine International* **3,** (2015).